# Low-temperature behavior of capture rate constants for inverse power potentials

E. I. Dashevskaya
*Department of Chemistry, Technion-Israel Institute of Technology, Haifa, 32000 Israel*

A. I. Maergoiz and J. Troe
*Institut für Physikalische Chemie der Universität Göttingen, Tammannstrasse 6, D-37077 Göttingen, Germany*

I. Litvin and E. E. Nikitin
*Department of Chemistry, Technion—Israel Institute of Technology, Haifa, 32000 Israel and Institut für Physikalische Chemie der Universität Göttingen, Tammannstrasse 6, D-37077 Göttingen, Germany*

(Received 23 September 2002; accepted 29 January 2003)

The energy dependence of the capture cross section and the temperature dependence of the capture rate constants for inverse power attractive potentials $V \propto -R^{-n}$ is considered in the regime where the quantum character of the relative motion of colliding partners is important. For practically interesting cases $n=4$ and $n=6$, a simple formula for the cross section is suggested which interpolates between the classical and the quantum Bethe limits. We have shown that the classical approximation for the capture cross section performs well far below the simple estimations of the onset the quantum regime. This seemingly ''classical'' feature of the cross section and the rate constant is due to the large quantum effects of the waves in transmission through and reflection above the centrifugal potential barriers. © *2003 American Institute of Physics.*
[DOI: 10.1063/1.1562159]

## I. INTRODUCTION

The rate of many barrierless chemical reactions is governed by the rate of complex formation (or capture) between the partners (see, e.g., Ref. 1). While the full quantum treatment of such events is the most general, some simplifications are possible under certain conditions. The most important are the fully classical treatment of the capture based on the classical (Cl) trajectory method, and adiabatic channel (AC) treatment.[2] The latter takes into account the quantum character of hindered rotational motion in the generally anisotropic potential between the partners but assumes that this motion is adiabatic with respect to the relative motion which in turn is regarded as classical. One can apply the following generalizations of the AC method that bring it closer to the full quantum treatment:

(i) an incorporation of nonadiabatic transitions between AC states in the regions of narrow avoided crossings;
(ii) an account for the axial nonadiabaticity (AN) from Coriolis coupling in the construction of ANAC potentials;
(iii) a quantum treatment of the relative motion of the partners.

While the points (i) and (ii) have been treated upon in Refs. 3 and 4, point (iii) has not been considered in full detail yet. Normally, quantum effects in the relative motion of partners are important only at such low temperatures that the rate constant is dominated by the contribution from the ground rovibronic state of the partners only. Even then, the capture event is complicated by the recoupling of the angular momenta in the collision process.[5] However, if the ground state is nondegenerate, there is only a single AC potential $V(R)$ that depends on the center-of-mass distance $R$ between the colliders; its long-range part determines the capture cross section, provided that the potential well depth is noticeably larger than the collision energy. Under this condition, the problem simplifies to the quantum capture of structureless particles. The physical processes that fall into this category, e.g., are the low-energy collisions of atomic ions in $S$ state with dipole or quadrupole diatoms in the ground rotational state, or the collisions of two dipole molecules, both in the ground rotational state. As explained in Refs. 3, 4, and 6, for the above three cases the long-range part of the AC potentials behave as $-C_{\mathrm{Lcd}}/R^4$, $-C_{\mathrm{Lcq}}/R^4$, $-C_{\mathrm{Wdd}}/R^6$, respectively, where the coefficients $C_{\mathrm{Lcd}}$, $C_{\mathrm{Lcq}}$, $C_{\mathrm{Wdd}}$ are certain combinations of the parameters of the Langevin+charge-dipole, Langevin+charge-quadrupole, and van der Waals+dipole–dipole interactions.

The problem of quantum capture was addressed in 1954 by Vogt and Wannier[7] for potentials behaving as $-1/R^4$. It was found that the quantum cross section under the condition of very low velocity $v \to 0$ is just twice the classical Langevin cross section. Later on, quantum effects in the capture were usually associated with the tunneling through the centrifugal barriers and the overbarrier reflection (see, e.g., the review by Clary[8] and the references cited therein). The importance of quantum effects for the Langevin interaction was estimated for different tunneling models in Ref. 9 with the conclusion that ''tunneling is unimportant unless the temperature becomes extremely low, and that overbarrier reflec-

 

tion exerts practically no effect on the capture rate.'' One therefore is tempted to use a simplified description of quantum effects in the capture by adopting the quantum expression for the cross section as a sum over the quantum numbers of orbital angular momentum $\ell$ and by using a step function for the barrier transmission coefficients. Within this approach one finds that, for the Langevin interaction, the capture rate constant diverges at low temperatures as $1/\sqrt{T}$.[9–13] This conclusion contradicts the results obtained by Vogt and Wannier.[7] More importantly, it also contradicts the low-energy Bethe limit which predicts an inverse dependence of the cross section on the collision velocity and therefore a limiting temperature-independent rate constant.[14] One should note that the inverse velocity law for inelastic (including capture) *s*-wave collision processes follows from the general analytical properties and unitarity of the scattering matrix[15] irrespective of the form of an interaction (in our case the capturing potential). Recently[16] an attempt was made to interpolate the energy dependence of the partial cross sections between their exact threshold value (Bethe threshold behavior for *s*-wave scattering,[14] the Wigner threshold behavior for higher angular momenta[16]) and an assumed high-energy dependence of these cross sections. However, one may object to this kind of approach since the accurate threshold behavior of the partial cross section with given quantum number $\ell$ is buried (except for $\ell=0$) under the heavy post-threshold, not-well-known weight of the preceding cross section with the quantum number $\ell-1$, see below.

With these remarks in mind, we reanalyze the problem by considering the simplest version of quantum capture collisions, when all complications related to the axial and radial nonadiabatic effects can be neglected, that is when the ground rovibronic state of the partners is nondegenerate and when possible contributions of excited rovibronic states can be disregarded. We consider quantum capture in the field of a general central potential $V(R)=-C_n/R^n$ with $n=4$ and 6. We derive a simple approximation for the low-temperature capture rate constant which later on can be compared with low-temperature treatments of cases where nonadiabatic effects are essential.

The plan of our presentation is the following: In Sec. II we review the results for classical capture in the field of $-1/R^n$ potentials. In Sec. III we discuss the Bethe limit of capture cross sections and rate constants for the same kind of potentials. In Sec. IV we present accurate numerical calculations for cross sections and energy-dependent rate coefficients. We suggest an analytical formula for the cross sections which bridges the gap between the classical regime and the Bethe limit. Section V gives the results for temperature-dependent rate constants. In Sec. VI our results are summarized and discussed. In the Appendix we also consider simple approximations to the capture rate coefficient which are based on analytical expressions for the barrier transmission coefficient.

## II. CLASSICAL CAPTURE CROSS SECTIONS AND RATE COEFFICIENTS

We consider the capture of two particles moving in the field of a central attractive potential of the form

$$V(R)=-C_n/R^n. \tag{1}$$

The classical capture cross section $\sigma_n^{\mathrm{Cl}}$ is expressed via the capture impact parameter $b_n$ or the corresponding angular momentum $L_n=pb_n$ (with $p$ being the linear momentum of relative motion, $p=\mu v$ with reduced mass $\mu$ and velocity $v$):

$$\sigma_n^{\mathrm{Cl}}=\pi b_n^2=\pi L_n^2/p^2. \tag{2}$$

For the potential in Eq. (1), one has (see, e.g., Ref. 18)

$$L_n(p)=p\left(\frac{\mu n C_n}{p^2}\right)^{1/n}\left(\frac{n}{n-2}\right)^{1/2-1/n}. \tag{3}$$

Besides the cross section $\sigma_n^{\mathrm{Cl}}$, we introduce the energy- (or momentum-) dependent capture rate coefficient

$$k_n^{\mathrm{Cl}}(p)=\mathrm{v}\sigma_n^{\mathrm{Cl}}(p). \tag{4}$$

From Eqs. (2), (3), and (4) we obtain

$$k_n^{\mathrm{Cl}}(p)=\begin{cases}\pi\left(\dfrac{8C_4}{\mu}\right)^{1/2} & \text{for} \quad n=4\\ 3\pi\left(\dfrac{C_6 p}{2\mu^2}\right)^{1/3} & \text{for} \quad n=6.\end{cases} \tag{5}$$

## III. BETHE CAPTURE CROSS SECTIONS AND RATE COEFFICIENTS

The general expression for the capture cross section in the case of spherically symmetric interaction is given by

$$\sigma_n^Q(k)=\sum_{\ell=0}^{\infty}\sigma_{\ell,n}^Q(k)=\frac{\pi}{k^2}\sum_{\ell=0}^{\infty}(2\ell+1)P_{\ell,n}(k), \tag{6}$$

where $k$ is the wave vector of relative motion ($k=p/\hbar$) and $P_{\ell,n}(k)$ is the capture probability for the $\ell$-partial wave cross section $\sigma_{\ell,n}^Q$. The Bethe limit is recovered from Eq. (6) when one retains only the contribution of *s*-wave scattering, and makes the scattering length approximation, i.e., $P_{0,n}(k)|_{k\to 0}=4\alpha_n'' k$ ($\alpha_n''$ being the imaginary part of the complex scattering length).[15] Within this approximation, Eq. (6) leads to

$$\sigma_n^Q(k)|_{k\to 0}\approx\sigma_n^{\mathrm{Bethe}}(k)=\frac{\pi}{k^2}P_{0,n}(k)|_{k\to 0}=\frac{4\pi\alpha_n''}{k}. \tag{7}$$

The condition $P_{0,n}(k)\ll 1$, under which Eq. (7) is valid, is one of the manifestations of the so-called suppression phenomena.[19,20] Physically, it is due to the low transmission of the impinging wave through a certain region of the potential where it begins to drop. The most simple description of this transmission corresponds to the case when the motion inside the well away from the above region is quasiclassical. Then the transmission and the absorption can be treated independently, and the capture probability $P_{\ell,n}$ can be identified with the transmission probability $T_{\ell,n}$. Under this condition, the transmission probability for the potential of the form in Eq. (1) can be found analytically:[21]

$$P_{0,n}(k)|_{k\to 0}=c_n R_{s,n} k, \tag{8}$$

where

$$R_{s,n}=(2\mu C_n/\hbar^2)^{1/(n-2)}$$

and

$$c_n=\left(\frac{1}{n-2}\right)^{2/(n-2)}\frac{4\pi}{\Gamma\left(\frac{1}{n-2}\right)\Gamma\left(1+\frac{1}{n-2}\right)}. \tag{9}$$

For the case of interest, $c_4=4$, $c_6=1.91$.

The conditions of small transmission over the potential drop and of the quasiclassical character of motion inside the well read

$$kR_{s,n}\ll 1 \quad \text{and} \quad R_{0,n}/R_{s,n}\ll 1, \tag{10}$$

where $R_{0,n}$ is the distance at which a long-range potential in Eq. (1) is noticeably modified by the short-range interaction. Note that the first inequality in Eq. (10) may be more restrictive than the condition for the capture cross section to be dominated by *s* wave scattering. From Eqs. (7) and (8) we get the following expressions for the Bethe cross section and the corresponding rate coefficient:

$$\sigma_n^{\text{Bethe}}(k)=\frac{\pi}{k}c_nR_{s,n} \quad \text{and} \quad k_n^{\text{Bethe}}=\frac{\pi\hbar}{\mu}c_nR_{s,n}. \tag{11}$$

By referring to Eq. (9), we see that $k_4^{\text{Bethe}}=2k_4^{\text{Cl}}$ in agreement with the results from Ref. 7.

## IV. BRIDGING BETWEEN THE BETHE LIMIT AND CLASSICAL REGIME FOR $n=4$ AND 6

For an accurate interpolation between the Bethe and classical limits, one has to calculate probabilities $P_{\ell,n}(\kappa)$ by numerically integrating the appropriate Schroedinger equation with an absorbing boundary condition at some small value of $R$ and relating the coefficients in the quasiclassical solutions for large and small $R$ (for large $R$ the motion is quasiclassical because it is free, for small $R$ the motion is quasiclassical according to our basic assumption, see Sec. II). The absorbing boundary condition inside the well eliminates any resonance features in the scattering; this principally distinguishes the capture event from any other event in which the reflected wave with a substantial amplitude exists inside the well (e.g., for the inelastic process of vibrational relaxation in atom–diatom collisions[22–24]). We calculate capture probabilities numerically for different $\ell$ within a range of $k$ which is wide enough to achieve the convergence of the quantum cross section to its classical limit. Beside giving numerically accurate cross sections and cross sections for the whole energy range, our objective was to see to what extent one can extrapolate classical cross section to low energies, what is the energy range for the validity of the Bethe approximation and the Wigner threshold law for the capture probability, and to derive a simple analytical formula for the capture cross section over a wide energy range. In the Appendix we also discuss some analytical approximations to the capture rate coefficients.

In solving the problem of the barrier transmission, we will use dimensionless distances $\rho=R/R_{s,n}$ and dimensionless vectors $\kappa=kR_{s,n}$. In these variables the Schroedinger equation reads

$$-\frac{d^2\psi_{\ell,\kappa}(\rho)}{2d\rho^2}+v_\ell^{\text{eff}}(\rho)\psi_{\ell,\kappa}(\rho)=\frac{\kappa^2}{2}\psi_{\ell,\kappa}(\rho), \tag{12}$$

where

$$v_\ell^{\text{eff}}(\rho)=\ell(\ell+1)/2\rho^2-1/2\rho^n. \tag{13}$$

Instead of the cross section in Eq. (6), we consider a scaled rate coefficient $\chi_n^{\text{Q}}(\kappa)$ which is proportional to $v\sigma_n^{\text{Q}}(\kappa)$:

$$\chi_n^{\text{Q}}(\kappa)=\sum_{\ell=0}^{\infty}\chi_{\ell,n}^{\text{Q}}(\kappa)=\frac{1}{2\kappa}\sum_{\ell=0}^{\infty}(2\ell+1)P_{\ell,n}(\kappa). \tag{14}$$

The classical counterpart of Eq. (14) is

$$\chi_n^{\text{Cl}}(\kappa)=\chi_n^{\text{Q}}(\kappa)|_{\kappa\gg 1}=\tilde{\ell}_n^2(\kappa)/2\kappa, \tag{15}$$

where $\tilde{\ell}_n(\kappa)=L_{c,n}(p)/\hbar$. For two cases of interest, we have $\tilde{\ell}_4(\kappa)=\sqrt{2\kappa}$ and $\tilde{\ell}_6(\kappa)=(3\sqrt{3}\kappa^2/2)^{1/3}$. In order to illustrate the successive contribution of different partial waves into the sum in Eq. (14), we use, instead of the wave vector $\kappa$, a related quantity $\lambda_n(\kappa)$. Functions $\lambda_n=\lambda_n(\kappa)$ are defined in such a way that every time, when the energy $\kappa^2/2$ equals the height of the centrifugal barrier for the effective potential in Eq. (13), $\lambda_n$ equals $\ell$. Namely, the relations between $\lambda_n$ and $\kappa$ are

$$\lambda_4(1+\lambda_4)=2\kappa, \quad \lambda_6(1+\lambda_6)=\left(\frac{3\sqrt{3}\kappa^2}{2}\right)^{2/3}. \tag{16}$$

Clearly, for $\kappa\gg 1$, $\lambda_n(\kappa)\to\tilde{\ell}_n(\kappa)$.

The scaled rate coefficients in the classical regime and in the Bethe limit read

$$\chi_n^{\text{Cl}}(\kappa)=\begin{cases}1, & n=4\\ \frac{3}{4}(2\kappa)^{1/3}, & n=6,\end{cases}$$
$$\chi_n^{\text{Bethe}}=\begin{cases}c_4/2=2, & n=4\\ c_6/2=0.956, & n=6,\end{cases} \tag{17}$$

respectively. Note that the numerical coefficient in front of the sum in Eq. (14) is chosen from the condition that $\chi_4^{\text{Cl}}=1$.

In what follows we present the results separately for the cases $n=4$ and $n=6$.

### A. Potential with $n=4$

Numerical transmission probability $P_{\ell,4}(\kappa)$ are presented in Fig. 1. The linear portions of the curves correspond to the Wigner law $P_{\ell,n}(\kappa)\propto\kappa^{2\ell+1}$,[17] the slopes of $\ln(P_{\ell,n})$ being equal to $2\ell+1$. We also see that, with increasing $\ell$, the Wigner behavior performs progressively better in the sense that it predicts the probabilities when they are not too low (the horizontal line in Fig. 1 corresponds to $P_{\ell,4}=1/2$). However, for *s*-wave scattering, the linear approximation for $P_{0,4}$ is valid within a disappointingly small range of $\kappa$, with the upper boundary being much lower than the contribution of the *p*-wave scattering. It is thus clear that for the calculation of the *s*-wave cross section one has to go beyond the scattering length approximation already for quite low energies. For approximate description of the transmission probability across the drop of the attractive potential, we can use

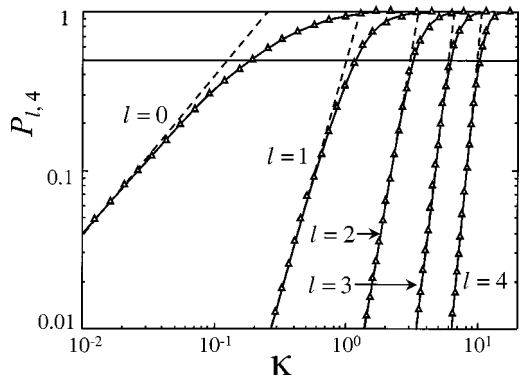


FIG. 1. Numerically determined probabilities $P_{\ell,4}(\kappa)$ vs $\kappa$. The linear parts of the plots correspond to the Wigner threshold law. The horizontal thick line corresponds to a probability of one-half, see text.

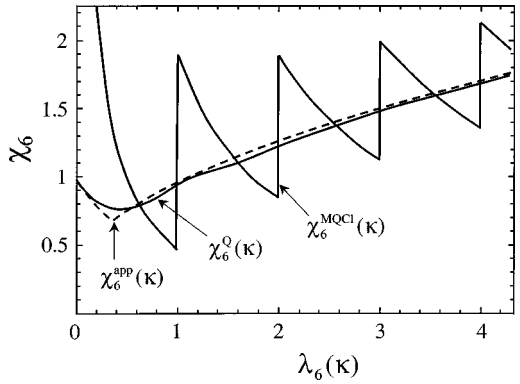


FIG. 3. Reduced rate coefficients $\chi_6^{Q}(\kappa)$, $\chi_6^{app}(\kappa)$, $\chi_6^{MQCl}(\kappa)$ vs $\lambda_6(\kappa)$, see text.

an analytical expression valid for an attractive exponential potential (see, e.g., Ref. 15). In doing so we will adjust the range of the exponential attraction in such a way as to ensure the correct Bethe limit. In this way we get

$$P_{0,4}(\kappa)\approx P^{app}(\kappa,c_4)=1-\exp(-c_4\kappa). \tag{18}$$

In Fig. 2, we present a plot of $\chi_4^{Q}(\kappa)$ versus $\lambda_4(\kappa)$. We see that $\chi_4^{Q}(\kappa)$ quite quickly reaches its classical limit (horizontal dashed line) oscillating about it with progressively decreasing amplitude. The quite small amplitude of oscillation is due to the compensation of the substantial tunneling and overbarrier reflection. However, at energies where the main contribution comes from the *s*-wave scattering (below the classical threshold for the *p*-wave scattering), the quantum rate coefficient significantly deviates from its classical counterpart. We can try to describe this deviation by combining the classical rate coefficient with the approximate *s*-wave rate coefficient by the following formula:

$$\chi_4^{app}(\kappa)=\max\{\chi_{0.4}^{Q,app}(\kappa),\chi_4^{Cl}(\kappa)\}, \tag{19}$$

where $\chi_{0,4}^{Q,app}(\kappa)$ is calculated with help of Eq. (18):

$$\chi_{0,4}^{Q}(\kappa)\approx\chi_{0,4}^{Q,app}(\kappa)=\frac{1}{2\kappa}\{1-\exp(-c_4\kappa)\}. \tag{20}$$

Figure 2 also shows the functions $\chi_4^{app}(\kappa)$, and $\chi_4^{MQCl}(\kappa)$; the latter is calculated according to Eq. (14) with

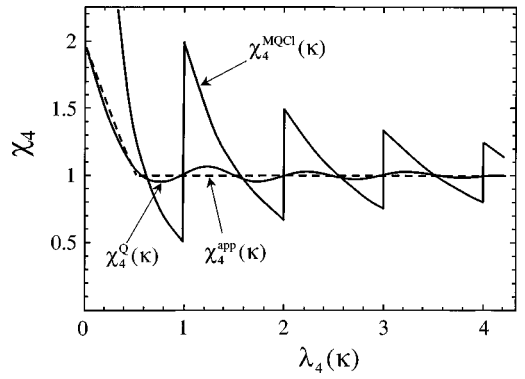


FIG. 2. Reduced rate coefficients $\chi_4^{Q}(\kappa)$, $\chi_4^{app}(\kappa)$, $\chi_4^{MQCl}(\kappa)$ vs $\lambda_4(\kappa)$, see text.

step functions $P_{\ell,4}(\kappa)=h[\kappa-\ell(\ell+1)/2]$. We see that a reasonable approximation to $\chi_4^{Q}(\kappa)$ is given by $\chi_4^{app}(\kappa)$ from Eq. (19) over the full range of $\kappa$. We expect that the relatively small discrepancy between the exact and approximate treatments will be even smaller after averaging the energy-dependent rate coefficient to produce the temperature-dependent rate constants. The modified quasiclassical (MQCl) approximation performs poorly, since it accounts neither for tunneling and overbarrier reflection for $\ell>0$ [this is the cause of the sawtooth structure in the $\chi_4^{MQCl}(\kappa)$ for $\kappa>1$], nor for the suppression for $\ell=0$ [this is the cause of the divergence of $\chi_4^{MQCl}(\kappa)\propto 1/\kappa$ for $\kappa<1$]. Finally, we note that the passage from the reduced rate coefficient to the rate coefficient in conventional units reads

$$k_c^{Q}(p)=K_4^{*}\times\chi_4^{Q}(p/p_4^{*}) \tag{21}$$

with $K_4^{*}=\pi(8C_4/\mu)^{1/2}$, $p_4^{*}=\hbar/R_{s,4}=(\hbar^4/2\mu C_4)^{1/2}$, and $R_{s,4}$ from Eq. (9).

### B. Potential with $n=6$

For the case $n=6$, the results are qualitatively similar to those for $n=4$, except for the fact that the asymptotic limit of the $\chi_6^{Q}(\kappa)$, i.e., $\chi_6^{Cl}(\kappa)$, now depends on $\kappa$, see Eq. (17). The plots of the three rate coefficients $\chi_6^{Q}(\kappa)$, $\chi_6^{app}(\kappa)$, $\chi_6^{MQCl}(\kappa)$, are shown in Fig. 3. We see again that the approximation of Eq. (19) reproduces accurate results because of the very strong tunneling and overbarrier reflection. We also note that, different from the case $n=4$, the rate coefficients for $n=6$ pass through a shallow minimum before the *p*-wave capture channel becomes classically open.

The rate coefficients in conventional units read

$$k_6^{Q}(p)=K_6^{*}\times\chi_6^{Q}(p/p_6^{*}) \tag{22}$$

with $K_6^{*}=(\pi/4)(C_6\hbar^2/8\mu^3)^{1/4}$, $p_6^{*}=\hbar/R_{s,6}=(\hbar^6/2\mu C_6)^{1/4}$, and $R_{s,6}$ from Eq. (9).

## V. TEMPERATURE-DEPENDENT RATE CONSTANTS FOR $n=4$ AND $n=6$

Temperature-dependent capture rate constants $\overline{\chi_n^{Q}}$ are obtained from $\chi_n^{Q}$ by averaging the latter over a Maxwell-Boltzmann velocity distribution. The distribution function *F*, written in terms of the variable $\kappa$, reads

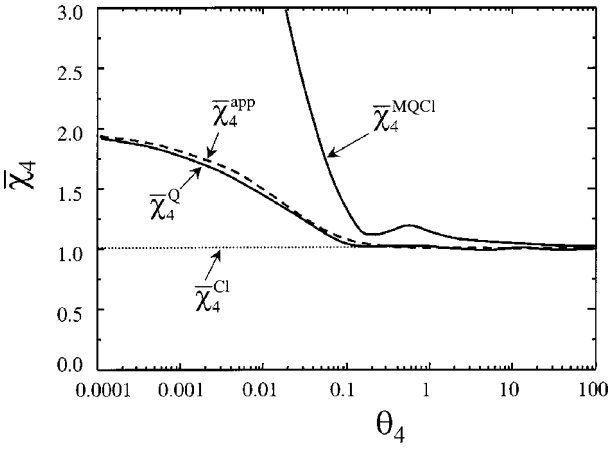


FIG. 4. Reduced rate constants $\overline{\chi}_4^{Q}(\theta_4)$, $\overline{\chi}_4^{app}(\theta_4)$, $\overline{\chi}_4^{MQCl}(\theta_4)$, $\overline{\chi}_4^{Cl}(\theta_4)$ vs $\theta_4$, see text.

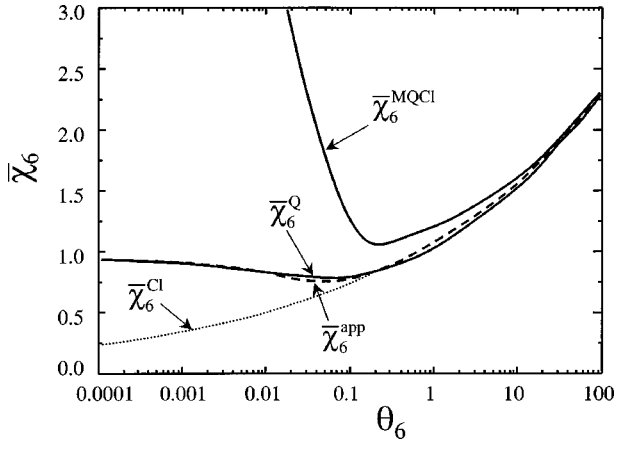


FIG. 5. Reduced rate constants $\overline{\chi}_6^{Q}(\theta_6)$, $\overline{\chi}_6^{app}(\theta_6)$, $\overline{\chi}_6^{MQCl}(\theta_6)$, $\overline{\chi}_6^{Cl}(\theta_6)$ vs $\theta_6$, see text.

$$F(\kappa;\theta_n)d\kappa=\frac{2\theta_n^{-3/2}}{\sqrt{2\pi}}\kappa^2\exp\left(-\frac{\kappa^2}{2\theta_n}\right)d\kappa, \tag{23}$$

where the reduced temperature $\theta_n$ is given by

$$\theta_n=k_BT\frac{\mu R_{s,n}^2}{\hbar^2}. \tag{24}$$

For $n=4$ and $n=6$, Eq. (24) corresponds to

$$\theta_4=(2C_4\mu^2/\hbar^4)k_BT \tag{25}$$

and

$$\theta_6=(2C_6\mu^3/\hbar^6)^{1/2}k_BT.$$

Temperature-dependent reduced rate constants $\overline{\chi}_n^{Q}(\theta_n)$ are defined, in a standard way, by

$$\overline{\chi}_n^{Q}(\theta_n)=\int_0^\infty\chi_n^{Q}(\kappa)F(\kappa,\theta_n)d\kappa. \tag{26}$$

The passage to conventional units is obtained through

$$\overline{k}_4^{Q}(T)=K_4^*\times\overline{\chi}_4^{Q}(T/T_4^*)\quad\text{with}\quad T_4^*=\hbar^4/2\mu^2C_4k_B \tag{27}$$

and

$$\overline{k}_4^{Q}(T)=K_6^*\times\overline{\chi}_4^{Q}(T/T_6^*)\quad\text{with}$$
$$T_6^*=\hbar^3/k_B(2C_6\mu^3)^{1/2},$$

where $K_4^*$ and $K_6^*$ are given by Eqs. (21) and (22), respectively. In order to see the significance of quantum corrections in the thermal rate constants, we also calculate $\overline{\chi}_n^{app}(\theta_n)$, $\overline{\chi}_n^{MQCl}(\theta_n)$, and $\overline{\chi}_n^{Cl}(\theta_n)$. These functions are presented in Fig. 4 for $n=4$ and in Fig. 5 for $n=6$. We see that the simple analytical approximation of Eq. (19) very well predicts the accurate rate constant, while $\overline{\chi}_n^{MQCl}(\theta_n)$ diverges as $1/\sqrt{\theta}$, and noticeably deviates from $\overline{\chi}_n^{Q}(\theta_n)$ and $\overline{\chi}_n^{app}(\theta_n)$ even at $\theta=\theta_{MQCl}\sim 10$. This value of $\theta_{MQCl}$ nicely agrees with an intuitive criterion for the onset of quantum effects, e.g., for $n=4$, $\theta_{MQCl}=10$ corresponds to $\kappa_{MQCl}^2=20$, which in turn corresponds to $\ell_{MQCl}=(4\kappa_{MQCl}^2)^{1/4}\approx 3$; this means that at $\theta_{MQCl}\approx 10$, about three partial waves contribute to the cross section, and 3 can be considered as already a ''large number.'' On the other hand, the deviations of $\overline{\chi}_4^{Q}(\theta)$ and $\overline{\chi}_4^{app}(\theta)$ from the classical rate constant $\overline{\chi}_4^{Cl}=1$ become noticeable at much lower temperatures, below, say, $\theta_Q\approx 0.1$. With $C_4\approx 1$ atomic units, $\mu=15$ atomic mass units $\approx 3\times 10^4$ atomic units, and the rough conversion factor $3\times 10^{-6}$ between Kelvin and atomic units, this value of $\theta_Q$ would correspond to $T_Q\approx 10^{-5}$ K for $n=4$ and $T_Q\approx 10^{-3}$ K for $n=6$. This difference in $T_Q$ for different $n$ is explained by the fact that the potential with higher $n$ is steeper and therefore the effect of quantum reflection from the potential drop is seen at higher $T$. For the same reason, $T_Q$ decreases with increasing interaction constant: the higher the interaction strength, the longer is the interfragment distance where the partners feel attraction, the more gradual is the potential drop, and the lower is the suppression.

A relevant example to this situation follows from the ion–dipole molecule interaction discussed by Troe.[6] The anisotropic interaction in this case becomes, in the AC description, a set of isotropic AC potentials with the interaction parameters determined by the Langevin (charge-induced dipole) parameters and second-order contributions from the rotational polarization (charge-permanent molecular dipole). For the ground rotational state of the molecule, there exists a single AC potential which has the form of Eq. (1) with $n=4$. The limiting classical low-temperature capture rate constant $(T\to 0)$ for this case reads

$$k=2\pi\sqrt{\alpha q^2/\mu}\sqrt{1+\mu_D^2/3\alpha B}, \tag{28}$$

where $q$ is the charge of the ion, $\alpha$ is the polarizability of the linear molecule, $\mu_D$ is its permanent dipole moment, and $B$ is its rotational constant. For a small value of the rotational constant, the coefficient $C_4$ [in Eq. (1)] in this case may strongly exceed the Langevin coefficient $q^2\alpha/2$. In other words, in this case $C_4$ may be noticeably higher than 1 a.u. such that $T_Q$ will be even lower than the above estimate of $10^{-5}$ K. The suggestion by Clary[8] that, for extremely low temperatures, the expression for the capture rate constant in the form of Eq. (28) should be multiplied by 2 is technically correct but therefore applies to extremely low temperatures only.

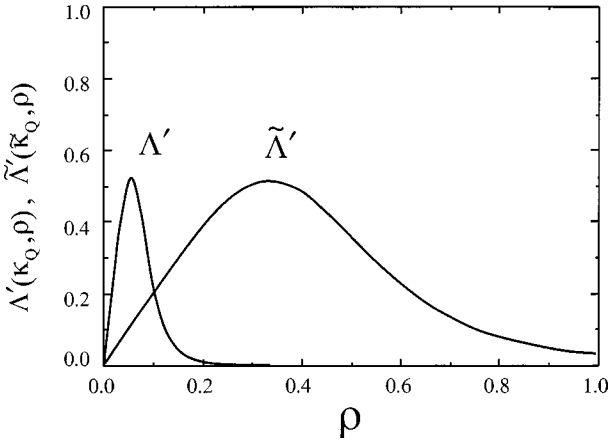


FIG. 6. Test for quasiclassical criteria. Curve 1 corresponds to $\Lambda'(\kappa_Q,\rho)$ for $\kappa_Q=150$, and curve 2 to $\tilde{\Lambda}'(\tilde{\kappa}_Q,\rho)$ for $\tilde{\kappa}_Q=4$, see text for more details.

According to our derivation, in general the values of $T_Q$ should be much lower than often assumed. For instance, a ''quantum threshold temperature'' for the system $CN+O_2$ was estimated as $T_Q\approx 7$ K in Ref. 16. In this estimation, an interaction of the type of Eq. (1) was assumed with $n=4$ (dipole-quadrupole interaction) and $C_4=8.6\times10^{-60}$ J m$^4$ $\approx 0.26$ a.u. In order to understand the origin of this large estimate of $T_Q$, we reexamine the criterion for the onset of quantum regime adopted in Ref. 16. The ''quantum threshold energy'' $E_Q$ or the ''quantum threshold temperature'' $T_Q=E_Q/k_B$ in Ref. 16 followed from a criterion $\max\{d\Lambda(E_Q,R)/dR\}=1/2$, instead of for the ''standard'' criterion[15] $\max\{d\tilde{\Lambda}(E_Q,R)/dR)\}\approx 1/2$, where $\Lambda(E,R)$ is the local de Broglie wavelength and $\tilde{\Lambda}=\Lambda/2\pi$ (for the detailed discussion of the application of the latter criterion to $R^{-n}$ potential see Ref. 21). Figure 6 shows the relevant plots in our dimensionless variables, namely $\Lambda'(\kappa_Q,\rho)=d\Lambda(\kappa_Q,\rho)/d\rho$ and $\tilde{\Lambda}'(\kappa_Q,\rho)=d\tilde{\Lambda}(\tilde{\kappa}_Q,\rho)/d\rho$ vs $\rho$ with $\Lambda=2\pi/\sqrt{\kappa^2+1/\rho^4}$, under the condition that the maximal values of these functions is about 1/2. For the criterion used in Ref. 16, we obtain $\kappa_Q\approx 150$ while the standard criterion yields $\tilde{\kappa}_Q\approx 4$. The latter value roughly corresponds to $\theta_Q\approx\tilde{\kappa}_Q^2/2\approx 8$, while the former corresponds to $\theta_Q\approx 10^4$. This difference by three orders of magnitudes in the estimates of the ''quantum threshold energy'' can therefore be attributed to the difference by the factor $2\pi$ in the two different quasiclassical criteria. An additional two orders of magnitude in $\theta_Q$ comes from the unexpectedly good performance of the classical approximation in the quantum regime. This explains the total difference of five orders of magnitude in $T_Q$ between the present results and those suggested in Ref. 16.

## VI. CONCLUSION

We have investigated the energy and the temperature ranges where capture cross sections and capture rate constants for inverse power potentials fall into the intermediate regime between the classical and the quantum Bethe limits. We have shown that tunneling and overbarrier reflection broaden the partial capture probabilities to such an extent that discrete structures of the cross sections are effectively lost and the classical (integral) expression for the cross section provides a very good approximation to the quantum cross section for collision energies even lower than the classical *p*-wave threshold. The use of a quantum summation over partial waves with neglect of tunneling and reflection, which is an often used procedure, definitely is inadequate and makes a false claim for a partial account of quantum effects. The *s*-wave scattering should be treated separately with proper account for the suppression effect; in turn, the suppression probability can be approximately recovered from the capture scattering length. The cross sections for classical capture and *s*-wave capture taken together allow one to construct a simple approximation to the quantum capture cross section over the whole energy or temperature range. Finally, we note that the Bethe limit of the rate constants is expected to be reached only at extremely low temperatures, below the $10^{-3}$-K range. This corresponds to a conclusion which also has been reached for the vibrational relaxation of molecules.[22–24] The present results correspond to reactions on uncoupled one-dimensional adiabatic channel potential curves for isotropic interaction. However, they apply equally well to such curves for anisotropic potentials. They provide a justification for the use of the semiclassical treatment in the statistical adiabatic channel model down to very low temperatures.[25] They are also of importance for future calculations of low-temperature rate constants for degenerate rovibronic states of colliders, since they permit us to skip the calculation of tunneling probabilities for the coupled channel potentials which, for degenerate rovibronic states, may have a quite complicated form.

## ACKNOWLEDGMENTS

Financial support of this work by the Deutsche Forschungsgemeinschaft (SFB 357 ''Molekulare Mechanismen unimolekularer Prozesse''), by the EU (TMR ''Astrophysical Chemistry''), and by the KAMEO, Israel, program are gratefully acknowledged.

## APPENDIX: ANALYTICAL APPROXIMATIONS FOR THE CAPTURE RATE COEFFICIENT

For illustrative purposes, in this Appendix simple approximations to the capture rate coefficient are also derived which are based on analytical expressions for the barrier transmission coefficient. We again consider the case $n=4$.

First we assume that the transmission probability is given by the expression appropriate for a particular case of the Eckart potential, the inverted Morse (IM) potential. The inverted Morse potential qualitatively resembles the centrifugal barrier and contains essentially two parameters, the height of the barrier $U_m$ and the characteristic length of the potential $a$. The transmission probability for the IM potential reads[15]

$$P^{\mathrm{IM}}(k)=\frac{2\sinh(ak)}{\exp(ak)+\exp(ak_{th})}, \tag{A1}$$

where $k_{th}$ is the wave vector that corresponds to $U_m$. Passing to the reduced wave vector $\kappa$ and identifying $\kappa_{th}$ with $\ell(\ell+1)/2$, we rewrite Eq. (A1) as

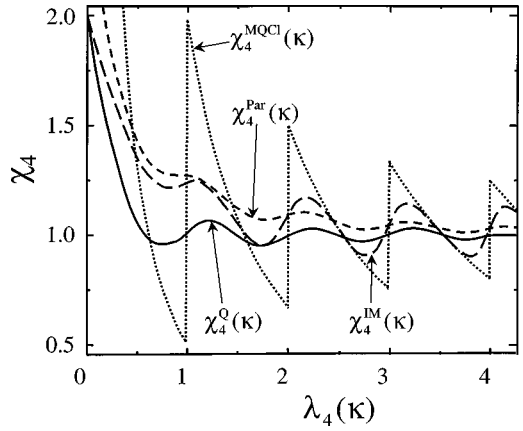


FIG. 7. Comparison of inverted Morse (IM) and parabolic (Par) approximations (dashed curves) with accurate quantum (Q) result (full curve) and modified quasiclassical (MQCl) approximation (dotted curve) for the reduced rate coefficient $\chi_4$.

$$P_{\ell,4}^{\mathrm{IM}}(\kappa)=\frac{2\sinh(\alpha\kappa)}{\exp(\alpha\kappa)+\exp[\alpha\ell(\ell+1)/2]}. \tag{A2}$$

In this equation, the scaling coefficient $\alpha$ can be found from various conditions. For instance, one may require that $P_{0,4}^{\mathrm{IM}}(\kappa)$ coincide with $P_{0,4}^{\mathrm{app}}(\kappa)$ from Eq. (18). This will yield $\alpha=c_4=4$. However, if this value of $\alpha$ is adopted, the capture rate coefficient

$$\chi_4^{\mathrm{IM}}(\kappa)=\frac{1}{2\kappa}\sum_{\ell=0}^{\infty}(2\ell+1)P_{\ell,4}^{\mathrm{IM}}(\kappa) \tag{A3}$$

at zero energy will be slightly higher than 2 because of the erroneous contributions of partial waves with $\ell>0$ [note that for small $\kappa$ all $P_{\ell,4}^{\mathrm{IM}}(\kappa)$ are proportional to $\kappa$ while the correct transmission probabilities are proportional to $\kappa^{2\ell+1}$]. Alternatively, one can choose the value of $\alpha$ such that $\lim_{\kappa\to 0}\chi_4^{\mathrm{IM}}(\kappa)=2$. This will make $\alpha$ lower than 4, namely $\alpha=3.3$. The plot of $\chi_4^{\mathrm{IM}}$ with the latter value of $\alpha$ is shown in Fig. 7 together with $\chi_4^{\mathrm{Q}}$ and $\chi_4^{\mathrm{MQCl}}$ versus $\lambda_4$.

Another simple treatment can be based on the parabolic approximation to the effective potential $v_\ell^{\mathrm{eff}}(\rho)$ near its maximum at $\rho=\rho_m$ as $v_\ell^{\mathrm{eff}}(\rho)\approx v_\ell^{\mathrm{par}}(\rho)$:

$$v_\ell^{\mathrm{eff}}(\rho)\approx v_\ell^{\mathrm{par}}(\rho)=\kappa_{\ell,4}^2/2-(\omega_\ell^2/2)(\rho-\rho_m)^2, \tag{A4}$$

where $\kappa_{\ell,4}$ is determined from Eq. (16) with $\lambda_4(\kappa_{\ell,4})=\ell$. Since the approximation $v_\ell^{\mathrm{eff}}(\rho)\approx v_\ell^{\mathrm{par}}(\rho)$ applies in the quasiclassical limit, $\omega_\ell$ is calculated by using the Langer correction to the centrifugal potential: $\omega_\ell=(\ell+1/2)^3/\sqrt{2}$. For the potential in Eq. (A4), a standard expression for $P_{\ell,4}^{\mathrm{par}}$ reads[15]

$$P_{\ell,4}^{\mathrm{Par}}(\kappa)=\frac{1}{1+\exp[(\pi/\omega_\ell)(\kappa_{\ell,4}^2-\kappa^2)]}. \tag{A5}$$

Making the linear expansion in the exponent in $\kappa-\kappa_{\ell,4}$ and changing the variable $\kappa$ into $\lambda_4$ we get

$$P_{\ell,4}^{\mathrm{par}}(\kappa)=\frac{1}{1+\exp[\sqrt{2}\pi(\ell-\lambda_4(\kappa))]}. \tag{A6}$$

We see that the total width $\Delta\lambda$ of the sigmoid-shaped function $P_{\ell,4}(\lambda_4)$ is about $2/(\pi\sqrt{2})$. It does not depend on $\ell$ and represents a noticeable fraction of the spacing between neighboring $\ell$ which is unity. Of course, Eq. (A6) cannot be used for $\ell=0$, and the transmission probability for the *s*-wave capture should be defined independently. We take it from Eq. (18) such that the expression for the scaled rate coefficient in the parabolic approximation becomes

$$\chi_4^{\mathrm{Par}}(\kappa)=\frac{P_{0,4}(\kappa)}{2\kappa}+\frac{1}{2\kappa}\sum_{\ell=1}^{\infty}(2\ell+1)P_{\ell,4}^{\mathrm{par}}(\kappa) \tag{A7}$$

with $P_{0,4}(\kappa)$ given by Eq. (18). The plot of $\chi_4^{\mathrm{Par}}$ is shown in Fig. 7.

We see that both the IM and parabolic approximations noticeably reduce the oscillatory behavior of the MQCl rate coefficient; they capture the essential features of the mutual compensation of tunneling and overbarrier reflection for partial waves with $\ell>1$. The IM approximation underestimates quantum effects of tunneling and overbarrier reflection, and shows significantly higher oscillatory behavior compared to the accurate dependence. The parabolic approximation accounts for the quantum effects near to the barrier maxima in a better way; therefore the cancellation of the two effects, reflection and transmission, is more substantial, and the oscillation amplitude is still smaller. However, the parabolic approximation suffers from a noticeable erroneous tunneling contribution at the foot of the barrier of the last classically closed channel. This explains the upward shift of the $\chi_4^{\mathrm{Par}}$ curve with respect to the $\chi_4^{\mathrm{Q}}$ curve. At very low energies, this shift leads to the $1/\kappa$ divergence that comes mainly from the incorrect *p*-wave tunneling capture [note that Eq. (A7) correctly describes the *s*-wave capture]. Still, this divergence is weaker than the $1/\kappa$ divergence of the incorrect *s*-wave capture within the MQCl treatment.

[1] J. Troe, J. Chem. Soc., Faraday Trans. **90**, 2303 (1994).
[2] M. Quack and J. Troe, in *Encyclopedia of Computational Chemistry*, edited by P. V. Schleyer, N. L. Allinger, T. Clark, J. Gasteiger, and P. A. Kollmann (Wiley, Chichester, UK, 1998), Vol. 4, p. 2708.
[3] E. E. Nikitin and J. Troe, Ber. Bunsenges. Phys. Chem. **101**, 445 (1997).
[4] A. I. Maergoiz, E. E. Nikitin, J. Troe, and V. G. Ushakov, J. Chem. Phys. **105**, 6263 (1996); **105**, 6270 (1996); **105**, 6277 (1996); **108**, 5265 (1998); **108**, 9987 (1998); **117**, 4201 (2002).
[5] E. E. Nikitin and J. Troe, J. Chem. Phys. **92**, 6594 (1990).
[6] J. Troe, J. Chem. Phys. **87**, 2773 (1987); **105**, 6249 (1996).
[7] E. Vogt and G. H. Wannier, Phys. Rev. **95**, 1190 (1954).
[8] D. C. Clary, Annu. Rev. Phys. Chem. **41**, 61 (1990).
[9] J. Turulski and J. Niedzielski, Int. J. Mass Spectrom. Ion Processes **139**, 155 (1994).
[10] J. Turulski and J. Niedzielski, Chem. Phys. **146**, 273 (1990).
[11] J. Turulski, J. Niedzielski, and K. Sakimoto, Chem. Phys. **174**, 387 (1993).
[12] A. Ratkiewicz, J. Turulski, and J. Niedzielski, Int. J. Mass Spectrom. Ion Processes **142**, 31 (1995).
[13] B. Pezler, J. Niedzielski, A. Ratkiewicz, and J. Turulski, Chem. Phys. **222**, 215 (1997).
[14] H. A. Bethe, Rev. Mod. Phys. **9**, 140 (1937).
[15] L. D. Landau and E. M. Lifshitz, *Quantum Mechanics* (Pergamon, Oxford, 1977).
[16] J. P. Hessler, J. Chem. Phys. **111**, 4068 (1999).

[17] E. P. Wigner, Phys. Rev. **73**, 1002 (1948).
[18] E. E. Nikitin, *Theory of Elementary Atomic and Molecular Processes in Gases* (Clarendon, Oxford, 1974).
[19] P. S. Julienne and F. H. Mies, J. Opt. Soc. Am. B **6**, 2257 (1989).
[20] R. Côté, E. J. Heller, and A. Dalgarno, Phys. Rev. A **53**, 234 (1996).
[21] R. Côté, H. Friedrich, and J. Trost, Phys. Rev. A **56**, 1781 (1997).
[22] D. W. Schwenke and D. G. Truhlar, J. Chem. Phys. **83**, 3454 (1985).
[23] N. Balakrishnan, R. C. Forrey, and A. Dalgarno, Phys. Rev. Lett. **80**, 3224 (1998).
[24] E. I. Dashevskaya and E. E. Nikitin, Phys. Rev. A **63**, 012711 (2000).
[25] A. I. Maergoiz, E. E. Nikitin, and J. Troe, J. Chem. Phys. **103**, 2083 (1995).